

Gravitational waves from MHD turbulence at the QCD phase transition as a source for Pulsar Timing Arrays

A. Roper Pol

*Université Paris Cité, CNRS, Astroparticule et Cosmologie, F-75013 Paris, France
School of Natural Sciences and Medicine, Ilia State University, GE-0194 Tbilisi, Georgia*



We propose that the recent observations reported by the different Pulsar Timing Array (PTA) collaborations (i.e. IPTA, EPTA, PPTA, and NANOGrav) of a common process over several pulsars could correspond to a stochastic gravitational wave background (SGWB) produced by turbulent sources in the early universe, in particular due to the magnetohydrodynamic (MHD) turbulence induced by primordial magnetic fields. I discuss recent results of numerical simulations of MHD turbulence and present an analytical template of the SGWB validated by the simulations. We use this template to constrain the magnetic field parameters using the results reported by the PTA collaborations. Finally, we compare the constraints on the primordial magnetic fields obtained from PTA with those from blazar signals observed by Fermi Large Area Telescope (LAT), from ultra high-energy cosmic rays, and from the cosmic microwave background. We show that a non-helical primordial magnetic field produced at the scale of the quantum chromodynamics phase transition is compatible with such constraints and it could additionally provide with a magnetic field at recombination that would help to alleviate the Hubble tension.

Contribution to the 2022 Gravitation session of the 56th Rencontres de Moriond.

1 Introduction

The field of gravitational astronomy is near its birth and has already led to astonishing discoveries. Starting in 2015 with the first detected gravitational wave event GW150914,¹ and the first multi-messenger detection GW170817 in 2017,² the LIGO-Virgo collaboration has recently released the second half of the third observing run O3b, with a total of 90 observed events.³ Many more are expected to come in the next few years and decades. In particular, magnetic fields and bulk fluid motions in the early universe can source a stochastic gravitational wave background (SGWB) of cosmological origin that can be generated, for example, during cosmological phase transitions.⁴ Depending on the energy scale at which the SGWB is produced, it will be present in a different range of frequencies within the gravitational spectrum. For example, a signal produced at the QCD phase transition with an energy scale $T_* \sim 100$ MeV could produce a SGWB at frequencies of a few nanohertz.⁵ It is precisely in the 1–100 nHz regime where pulsar timing arrays (PTA) seek to detect GWs by monitoring the time-delay signals of an array of millisecond pulsars. Recently, the North American Nanohertz Observatory for Gravitational Waves (NANOGrav), after 12.5 years of observations, has reported a common-

spectrum process, although the statistical significance of a quadrupolar correlation (i.e. following the Hellings-Downs curve as expected for GW signals⁶) is still not conclusive.⁷ Similar results from the Parkes Pulsar Timing Array (PPTA),⁸ the European Pulsar Timing Array (EPTA),⁹ and the International Pulsar Timing Array (IPTA) collaborations¹⁰ followed, using data from pulsars that span a total duration of 15, 24, and 31 years, respectively. Different sources of GWs that would yield a SGWB compatible with the common-process observed by the PTA collaborations have been proposed. The most studied source is astrophysical and corresponds to the SGWB produced by a population of merging supermassive black hole binaries.¹¹ Alternatively, cosmological sources have been proposed: inflation,¹² cosmic strings and domain walls,¹³ primordial black holes,¹⁴ supercooled and dark phase transitions,¹⁵ the QCD phase transition, and primordial magnetic fields.¹⁶ I present hereby the latter scenario, where a primordial magnetic field produced or present during the QCD phase transition yields a SGWB that is compatible with the observations reported by the PTA collaborations.^{16,17,18} In particular, I present the results of Roper Pol et al. 2022.¹⁸

2 MHD turbulence and gravitational wave production

In the presence of magnetic fields, due to the high-conductivity in the early universe, the plasma velocity field is highly coupled to the primordial magnetic field, leading inevitably to the development of magnetohydrodynamic (MHD) turbulence.¹⁹ On the other hand, the anisotropic stresses due to the velocity and magnetic fields lead to the production of GWs. To compute the resulting SGWB, one needs to solve the full system of MHD equations. We have performed such numerical simulations in a recent publication¹⁸ using the PENCIL CODE²⁰ and following a similar setup than previous simulations of MHD turbulence production of GWs from cosmological phase transitions.^{17,21,22,23,24,25} The numerical setup and methodology, and some of these results, in particular focusing on the electroweak phase transition and the potential detectability of polarization in the SGWB, were presented during the Gravitation session of the 55th Rencontres de Moriond.²⁶

The tensor-mode perturbations h_{ij}^{phys} above the Friedmann-Lemaître-Robertson-Walker background metric tensor are described by the GW equation. During the radiation-dominated era, it reads

$$(\partial_t^2 - \nabla^2) h_{ij} = 6 \Pi_{ij}/t, \quad (1)$$

for scaled strains $h_{ij} = ah_{ij}^{\text{phys}}$, comoving coordinates and stress tensor components, and conformal time. We have used a normalization appropriate for numerical simulations,^{21,22} and $\tilde{\Pi}_{ij} = \Lambda_{ijlm} \tilde{T}_{lm}$ (where a tilde indicates Fourier space) corresponds to the traceless-transverse projection of the stress-energy tensor produced by the MHD turbulence,

$$T_{ij} = (p/c^2 + \rho)\gamma^2 u_i u_j - B_i B_j + \delta_{ij} B^2/2, \quad (2)$$

where $\Lambda_{ijlm} = P_{il} P_{jm} - \frac{1}{2} P_{ij} P_{lm}$ and $P_{ij} = \delta_{ij} - \hat{k}_i \hat{k}_j$ are projection operators.

2.1 Numerical results

We solve the MHD equations numerically and construct the stress tensor Π_{ij} ; see eq. (2). Then, we compute the resulting GW radiation solving eq. (1). For this purpose, we use the open-source PENCIL CODE.

We set as initial condition of the simulations a fully-developed non-helical MHD spectrum for the magnetic field, and zero initial bulk velocity, present at the QCD phase transition (in general, at an energy scale T_*) with a characteristic scale k_* , given as a fraction of the Hubble scale, and a characteristic strength Ω_M^* , given as a fraction of the critical energy density. We chose this initial condition for two main reasons. In first place, it is conservative: whatever the

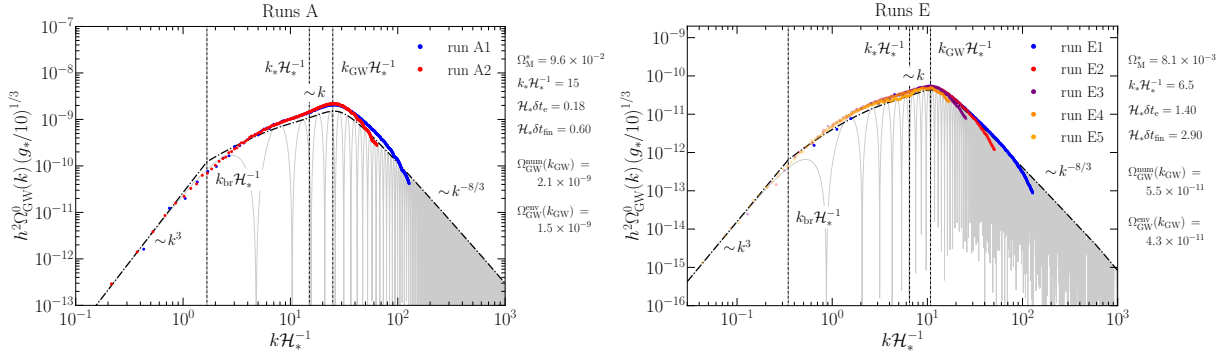


Figure 1 – SGWB spectrum produced by MHD turbulence driven by non-helical magnetic fields at the QCD phase transition, computed numerically using the PENCIL CODE (colored dots), and obtained from an analytical template (solid lines) and its envelope (dash-dotted lines). The left panel shows a series of runs with a short eddy turnover time (18% of one Hubble time) and the right panel shows a series of runs with a long eddy turnover time (1.4 Hubble times). The specific parameters of each run and the results can be found in Roper Pol et al. 2022.¹⁸

initial generation mechanism, the magnetic field is expected to enter a phase of fully developed and freely decaying turbulence.¹⁹ Any initial phase of magnetic field growth would increase the GW production.^{22,23,25} Secondly, simple initial conditions make it easier to build an analytical description of the simulation outcome. Since we want to model magnetically driven turbulence, we also neglect the presence of initial bulk velocity for simplicity. The resulting SGWBs computed from the numerical simulations are shown in figure 1.

2.2 Analytical SGWB template

In general, the simulations show that the SGWB evolves with a characteristic time scale $\delta t_{\text{GW}} \sim 1/k_*$, while the magnetic field evolution is determined by the eddy turnover time, $\delta t_e = (v_A k_*)^{-1}$, where v_A is the Alfvén speed. Hence, due to causality, $\delta t_{\text{GW}}/\delta t_e \sim v_A < 1$. This reasoning motivates the assumption that the anisotropic stresses are constant in time, which simplifies the solution to the GW equation; see eq. (1). In particular, the envelope of the resulting SGWB spectrum, derived in Roper Pol et al. 2022,¹⁸ is

$$\Omega_{\text{GW}}(k, t_*) \approx 3 \left(\frac{k}{k_*} \right)^3 \Omega_{\text{M}}^* \frac{\mathcal{C}(\alpha)}{\mathcal{A}^2(\alpha)} p_{\Pi} \left(\frac{k}{k_*} \right) \begin{cases} \ln^2[1 + \mathcal{H}_* \delta t_{\text{fin}}] & \text{if } k \delta t_{\text{fin}} < 1, \\ \ln^2[1 + (k/\mathcal{H}_*)^{-1}] & \text{if } k \delta t_{\text{fin}} \geq 1. \end{cases} \quad (3)$$

The SGWB shows a dependence with the square of the magnetic field strength Ω_{M}^* and the magnetic spectral shape via $p_{\Pi}(k/k_*)$. In this work, we consider an initial magnetic spectrum given as a smoothed broken power law, following a Batchelor spectrum $\sim k^4$ at large scales, and a Kolmogorov spectrum $\sim k^{-5/3}$ at small scales, with $\alpha = 2$ determining the smoothness of the transition; see eq. (6) of Roper Pol et al. 2022.¹⁸ The parameters \mathcal{C} and \mathcal{A} are numerical values that depend on α , and p_{Π} is given by the projection of the convolution of the magnetic spectrum for Gaussian magnetic fields; see eq. (11) of Roper Pol et al. 2022.¹⁸ In this expression, we have considered an effective duration of the turbulence sourcing δt_{fin} that can not be predicted by the analytical model. We expect that this duration is proportional to the time scale of the magnetic evolution, i.e. the eddy turnover time. Hence, we use the results from the numerical simulations to provide the empirical fit $\delta t_{\text{fin}} = 0.184 \mathcal{H}_*^{-1} + 1.937 \delta t_e$. Figure 1 compares the analytical model with the results from the numerical simulations, and shows that the envelope of the analytical template is an accurate representation of the numerical results.¹⁸

3 Constraints on the magnetic field

Once that we have derived an analytical template of the SGWB produced by MHD turbulence due to the presence of a non-helical magnetic field in the early universe, which has been validated

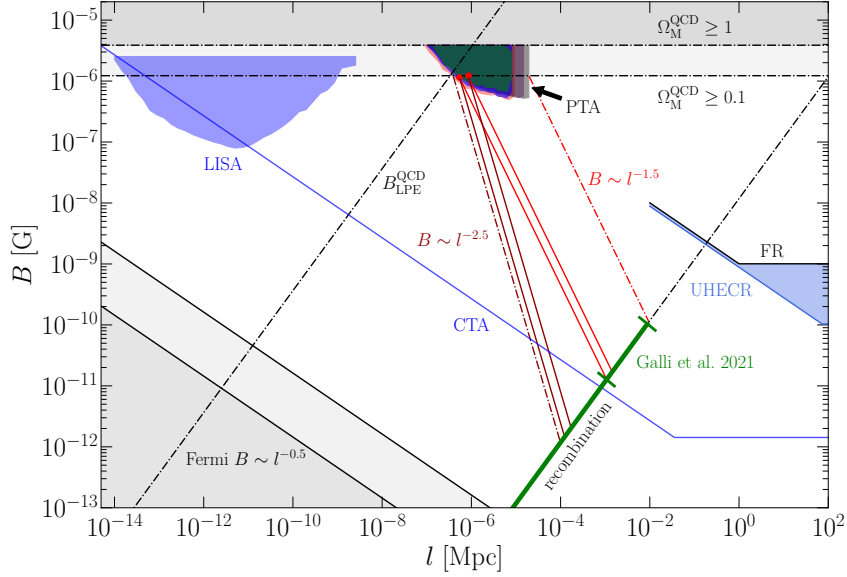


Figure 2 – Magnetic field amplitude B and length at the spectral peak l given as present time observables (i.e. in comoving units) compatible with the observations from PTA compared to the different constraints on primordial magnetic fields. The red and brown lines indicate possible evolutionary paths of the primordial magnetic field from its generation down to recombination. For details, see Fig. 7’s caption in Roper Pol et al. 2022.¹⁸

by the simulations, we can compare the resulting SGWB to the observations reported by the different PTA collaborations,^{7,8,9,10} thereby inferring the range of parameters T_* , k_* , and Ω_M^* that could account for the PTA results. The details and results of this analysis are described in Roper Pol et al. 2022.¹⁸ Figure 2 shows the range of parameters k_* and Ω_M^* , for the compatible range of energy scales T_* , that are compatible with the results of the different PTA collaborations. They are shown in terms of the magnetic field amplitude B (in Gauss) and the length scale of the spectral peak l (in Mpc), as observables at present time.¹⁸ Such magnetic fields will continue to evolve following MHD turbulent free decay down to recombination, when the magnetic fields become frozen-in and only evolve following the expansion of the universe afterwards.²⁷ Figure 2 shows that the magnetic fields compatible with the observations from the PTA collaborations are also compatible with constraints on large-scale magnetic fields from the Fermi collaboration,²⁸ constraints from ultra-high-energy cosmic rays (UHECR),²⁹ constraints from Faraday Rotation (FR),³⁰ and constraints from the cosmic microwave background (CMB).³² In fact, the resulting primordial magnetic field from the PTA observations is also compatible with the constraints proposed by Jedamzik & Pogosian 2020,³¹ updated recently by Galli et al. 2022,³² which allow a CMB value of the current Hubble rate $H_0 \approx 70 \text{ km s}^{-1} \text{ Mpc}^{-1}$, hence relieving the Hubble tension.

4 Conclusions

I have presented recent results on the SGWB produced by MHD turbulence driven by primordial magnetic fields from the radiation-dominated early universe. New MHD numerical simulations allowed us to study the relevant dynamical range of the GW spectrum and to validate an analytical template of the SGWB that holds under the assumption of constant-in-time anisotropic stresses. Whether the PTA observations are confirmed to correspond to a SGWB (i.e. if the correlation between pulsars is confirmed to follow the Hellings-Downs curve) in the future, they could potentially correspond to a SGWB produced by primordial magnetic fields with a magnetic energy density of at least 1% the radiation energy density and a characteristic length scale within 10% of the horizon scale. The energy scale is constrained to be between 1 and 200 MeV and hence, the signal could correspond to a primordial magnetic field produced during the QCD

phase transition. The analytical model developed, validated by the simulations, allowed us to predict where the position of the break from f^3 to f appears within the SGWB. This break, if observed in future PTA data, could help to elucidate among an astrophysical or cosmological origin of the SGWB signal.¹⁸

Acknowledgments

I would like to acknowledge my collaborators C. Caprini, A. Neronov and D. Semikoz for their fruitful contributions to this work. Support through the French National Research Agency (ANR) project MMUniverse (ANR-19-CE31-0020) and the Shota Rustaveli National Science Foundation of Georgia (grant FR/18-1462) are gratefully acknowledged. I thank the *Rencontres de Moriond* organizers to give me the chance to present this work and to the rest of participants for providing a great environment and interesting discussions during the meeting.

References

1. B. P. Abbott *et al.* [LIGO Scientific and Virgo], *Phys. Rev. Lett.* **116**, 061102 (2016).
2. B. P. Abbott *et al.* [LIGO Scientific and Virgo], *Phys. Rev. Lett.* **119**, 161101 (2017).
3. R. Abbott *et al.* [LIGO Scientific, VIRGO and KAGRA] (2021) [arXiv:2111.03606 [gr-qc]].
4. C. Caprini and D. G. Figueroa, *Class. Quant. Grav.* **35**, 163001 (2018).
5. D. V. Deryagin, D. Y. Grigoriev, V. A. Rubakov and M. V. Sazhin, *Mod. Phys. Lett. A* **1**, 593-600 (1986).
6. R. W. Hellings and G. S. Downs, *Astrophys. J. Lett.* **265**, L39-L42 (1983).
7. Z. Arzoumanian *et al.* [NANOGrav], *Astrophys. J. Lett.* **905**, L34 (2020).
8. B. Goncharov, R. M. Shannon, D. J. Reardon, G. Hobbs, A. Zic, M. Bailes, M. Curylo, S. Dai, M. Kerr and M. E. Lower, *et al. Astrophys. J. Lett.* **917**, L19 (2021).
9. S. Chen, R. N. Caballero, Y. J. Guo, A. Chalumeau, K. Liu, G. Shaifullah, K. J. Lee, S. Babak, G. Desvignes and A. Parthasarathy, *et al. Mon. Not. Roy. Astron. Soc.* **508**, 4970-4993 (2021).
10. J. Antoniadis, Z. Arzoumanian, S. Babak, M. Bailes, A. S. B. Nielsen, P. T. Baker, C. G. Bassa, B. Bcsy, A. Berthereau and M. Bonetti, *et al. Mon. Not. Roy. Astron. Soc.* **510**, 4873-4887 (2022).
11. M. G. Haehnelt, *Mon. Not. Roy. Astron. Soc.* **269**, 199 (1994).
12. S. Vagnozzi, *Mon. Not. Roy. Astron. Soc.* **502**, L11-L15 (2021).
13. J. Ellis and M. Lewicki, *Phys. Rev. Lett.* **126**, 041304 (2021).
14. V. Vaskonen and H. Veermäe, *Phys. Rev. Lett.* **126**, 051303 (2021).
15. Y. Nakai, M. Suzuki, F. Takahashi and M. Yamada, *Phys. Lett. B* **816**, 136238 (2021).
16. A. Neronov, A. Roper Pol, C. Caprini and D. Semikoz, *Phys. Rev. D* **103**, 041302 (2021).
17. A. Brandenburg, E. Clarke, Y. He and T. Kahniashvili, *Phys. Rev. D* **104**, 043513 (2021).
18. A. Roper Pol, C. Caprini, A. Neronov and D. Semikoz, *Phys. Rev. D*, *in press* (2022) [arXiv:2201.05630 [astro-ph.CO]].
19. J. Ahonen and K. Enqvist, *Phys. Lett. B* **382**, 40-44 (1996).
20. A. Brandenburg *et al.* [Pencil Code], *J. Open Source Softw.* **6**, 2807 (2021).
21. A. Roper Pol, A. Brandenburg, T. Kahniashvili, A. Kosowsky and S. Mandal, *Geophys. Astrophys. Fluid Dynamics* **114**, 130 (2020).
22. A. Roper Pol, S. Mandal, A. Brandenburg, T. Kahniashvili and A. Kosowsky, *Phys. Rev. D* **102**, 083512 (2020).
23. T. Kahniashvili, A. Brandenburg, G. Gogoberidze, S. Mandal and A. Roper Pol, *Phys. Rev. Res.* **3**, 013193 (2021).
24. A. Brandenburg, G. Gogoberidze, T. Kahniashvili, S. Mandal, A. Roper Pol and N. Shenoy, *Class. Quant. Grav.* **38**, 145002 (2021).

25. A. Roper Pol, S. Mandal, A. Brandenburg and T. Kahniashvili, *JCAP* **04** (2022), 019.
26. A. Roper Pol, ARISF, ISBN:979-10-96879-14-4 (2021) [arXiv:2105.08287 [gr-qc]].
27. R. Durrer and A. Neronov, *Astron. Astrophys. Rev.* **21**, 62 (2013).
28. A. Neronov and I. Vovk, *Science* **328**, 73 (2010).
29. R. U. Abbasi *et al.* [Telescope Array] (2021) [arXiv:2110.14827 [astro-ph.HE]].
30. M. S. Pshirkov, P. G. Tinyakov and F. R. Urban, *Phys. Rev. Lett.* **116**, 191302 (2016).
31. K. Jedamzik and L. Pogosian, *Phys. Rev. Lett.* **125**, 181302 (2020).
32. S. Galli, L. Pogosian, K. Jedamzik and L. Balkenhol, *Phys. Rev. D* **105**, 023513 (2022).